ADVANCED MATERIALS
www.advmat.de

www.MaterialsViews.com

Nanoimprinted Organic Semiconductor Laser Pumped by a Light-Emitting Diode

Georgios Tsiminis, Yue Wang, Alexander L. Kanibolotsky, Anto R. Inigo, Peter J. Skabara, Ifor D. W. Samuel, and Graham A. Turnbull**

Organic semiconductors exhibit several attractive features as visible laser media, such as broad absorption and emission spectra, high optical-gain coefficients and simple processing from solution.[1–3] There has been significant progress in the development of organic semiconductor lasers, with applications now emerging, such as integrated light sources for spectroscopy[4–6] and vapor sensors.[7,8] A significant limitation to their practical application has been the requirement for a complex, expensive laser to optically pump the organic laser, until the demonstration of laser-diode pumping,[9–12] and more recently the breakthrough of LED pumping.[13] These advances now make it timely and important to develop simple, scalable fabrication of organic lasers that is compatible with inexpensive batch-processed LED pump sources.

The most widely developed organic semiconductor lasers are distributed feedback resonators,[1,14,15] which require nanopatterned substrates with features ≈100 nm. Such resonators are commonly made by complex processes such as electron-beam lithography and holography, followed by chemical etching. Alternative promising approaches for such nanofabrication include nanoimprint lithography (NIL)[16,17] and even direct optical writing.[18] NIL has been used to produce roll-to-roll flexible optics[19] and optoelectronics,[20] and therefore offers great potential for simple mass-production of organic semiconductor lasers. While the feasibility of producing organic lasers using nanoimprint techniques has been demonstrated,[5,15,21–27] the resulting lasers have shown threshold excitation densities of typically 8 kW cm^{-2} [23,28,29] and higher, or have required UV excitation,[26] and therefore necessitate a laser pump source.

In this paper, we report a tunable organic semiconductor laser fabricated by UV-nanoimprint lithography (UV-NIL) that can be pumped by a pulsed inorganic LED. We optimize the molecular weight distribution of a low-threshold polymer gain medium, the optical design of the resonator and the pump excitation area; each of which strongly influence the laser threshold density.[30] We thereby show that it is possible to demonstrate nanoimprinted lasers that are directly powered by a single LED. The use of this simple pump source is a direct consequence of the very low lasing threshold of 0.77 kW cm^{-2}, the first time a UV-NIL organic laser has been demonstrated to have a threshold density below 8 kW cm^{-2}. While the first example of an LED-pumped organic laser used a resonator fabricated by holography and chemical etching,[13] this result shows the potential for making tunable organic lasers that could be mass produced at low cost, including an integrated excitation LED, thus making them a realistic compact coherent light source.

Poly(2,5-bis(2',5'-bis(2"-ethylhexyloxy)phenyl)-*p*-phenylenevinylene) (BBEHP-PPV) was chosen as the gain medium for the lasers. This polymer (**Figure 1**) has previously been shown to exhibit a low lasing threshold, and has been applied as an explosive vapor sensor.[7] It is an attractive candidate for LED

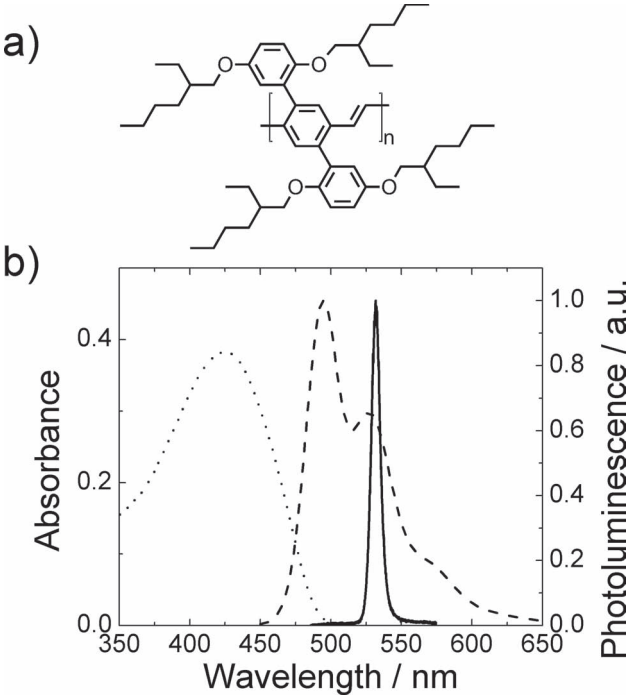

Figure 1. a) Chemical structure of BBEHP-PPV. b) Absorption (dotted line), photoluminescence (dashed line) and amplified spontaneous emission (solid line) spectra for a thin film of BBEHP-PPV.

Dr. G. Tsiminis,[+] Y. Wang,[+] Prof. I. D. W. Samuel, Dr. G. A. Turnbull
Organic Semiconductor Centre
SUPA, School of Physics & Astronomy
University of St Andrews
St Andrews, KY16 9SS, UK
E-mail: idws@st-andrews.ac.uk, gat@st-andrews.ac.uk
Dr. A. L. Kanibolotsky, Dr. A. R. Inigo, Prof. P. J. Skabara
WestCHEM, Department of Pure and Applied Chemistry
University of Strathclyde
295 Cathedral Street, Glasgow, G1 1XL, UK
[+]These authors contributed equally to this work.

DOI: 10.1002/adma.201205096

excitation due to its strong absorption around 450 nm matching the wavelength of the highest power commercial LEDs.

The optical properties of conjugated polymers can depend strongly upon molecular weight.[31] In order to optimize the gain medium for lowest threshold operation we therefore first studied the influence of molecular weight and polydispersity on the emission efficiency and optical gain in BBEHP-PPV. The polymer was synthesized by a slightly modified procedure from that previously reported[7] and was then further refined using Soxhlet extraction with methanol, acetone and dichloromethane to yield fractions of lower polydispersity. Properties of the eight samples of BBEHP-PPV (labeled **1** to **8** in order of weight-average molecular weight (M_w)) are summarized in **Table 1**. The polymers after Soxhlet extraction have lower polydispersity compared with the as-synthesised polymer (**4**, **7**) while the acetone extraction **1** yielded a monodisperse sample of significantly lower molecular weight than other samples.

Absorption and photoluminescence spectra, as well as photoluminescence quantum yield (PLQY) values were measured for films of each sample. Figure 1 shows typical absorption and PL spectra for a film of 150 nm thickness. The peak absorption was at 426 nm and the photoluminescence had two peaks at 495 nm (0–0 transition) and 527 nm (0–1 transition). The films made from all samples have high PLQY, mostly above 80% (Table 1), suggesting that there is little aggregation affecting the emission from any of the BBEHP-PPV films.

Optical gain in BBEHP-PPV waveguides was assessed by measuring amplified spontaneous emission (ASE) in the films under nanosecond pulsed excitation. The films (≈350 nm thickness) were optically pumped at a wavelength of 430 nm with a stripe of length 4 mm and the emission was measured from the end of the stripe. Above a threshold pumping intensity, gain narrowed emission (Figure 1) was observed from each sample, with a peak wavelength of 532 ± 2 nm and a linewidth (full width at half maximum) of 7 ± 1 nm. Table 1 and **Figure 2** give details of the measured ASE thresholds of each sample, and their relation to molecular weight and polydispersity.

Most samples had remarkably low ASE thresholds in the range of 170 to 300 W cm^{-2}, with two samples having significantly higher ASE thresholds. These were the monodisperse lowest molecular weight sample **1**, and the high molecular weight sample **8** that was extracted as fibres. Films spin-cast from these two samples were typically of lower quality, and had slightly higher surface roughness (typical atomic force microscopy (AFM) images are given in Figure S1 in the Supporting Information), which would lead to increased waveguide scattering loss. In addition, the maximum film thickness that could be spin cast with the lowest M_w sample **1** was only 150 nm, half the thickness of the other films, and thus lower optical confinement of the waveguided mode would also increase the threshold.[32] For the samples of intermediate molecular weight, there is a weak trend of lower threshold for lower M_w and polydispersity. As the PLQYs are consistently high this trend may be due to a difference in waveguide loss, shown previously to depend on M_w for MEH-PPV, a similar light-emitting polymer.[31] Waveguide transmission losses were measured for the films by increasing the propagation length of ASE to the edge of the film. Measured losses for films with 300k < M_w < 600k g mol^{-1} were very low, typically less than 2 cm^{-1} (Table 1), but did not show a resolvable trend.

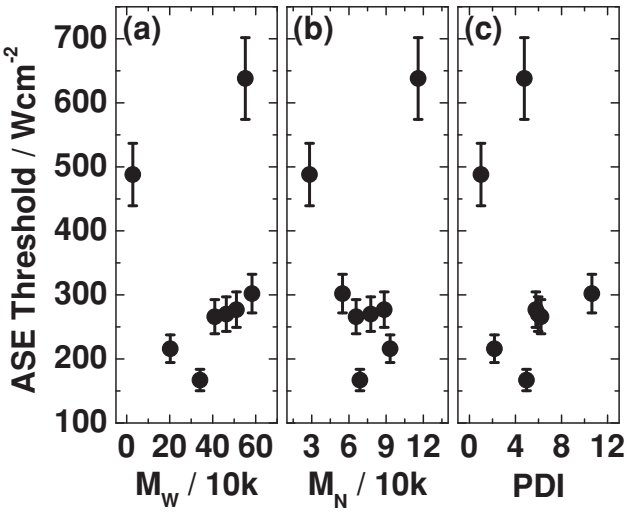

Figure 2. ASE threshold dependence of: a) weight-average molecular weights (M_w), b) number-average molecular weights (M_n) and c) polydispersity index (PDI) of different samples of BBEHP-PPV polymers.

Table 1. Molecular weight, polydispersity and photophysical data for the eight samples of BBEHP-PPV studied. The polymer was synthesized in four batches (**a** to **d**), from which samples with a range of molecular weights were obtained by reprecipitation or by Soxhlet extraction. Samples **1** to **8** are listed by appearance and then in order of increasing M_w. Waveguide loss was not measured for polymer batch **b**.

Sample number	Isolation Method (from synthesis batch)	Appearance	M_w [g mol^{-1}]	M_n [g mol^{-1}]	PDI	PLQY [%]	ASE threshold [W cm^{-2}]	Waveguide loss [cm^{-1}]
1	Soxhlet, acetone (batch **c**)	Powder	28 430	28 270	1.01	82	488	1.5 ± 0.5
2	Soxhlet, CH_2Cl_2 (batch **d**)	Powder	202 800	93 220	2.18	81	216	2 ± 2
3	Soxhlet, CH_2Cl_2 (batch **d**)	Powder	341 300	68 860	4.96	84	167	1.3 ± 0.5
4	Reprecipitation (batch **b**)	Powder	409 700	65 840	6.22	88	266	-
5	Soxhlet, CH_2Cl_2 (batch **c**)	Powder	463 300	77 570	6.0	77	270	0.8 ± 0.5
6	Soxhlet, CH_2Cl_2 (batch **b**)	Powder	510 400	88 470	5.77	86	277	-
7	Reprecipitation (batch **a**)	Powder	582 800	54 790	10.6	82	302	0.6 ± 0.5
8	Soxhlet, CH_2Cl_2 (batch **d**)	Fiber	551 800	115 800	4.77	84	638	2.4 ± 0.5

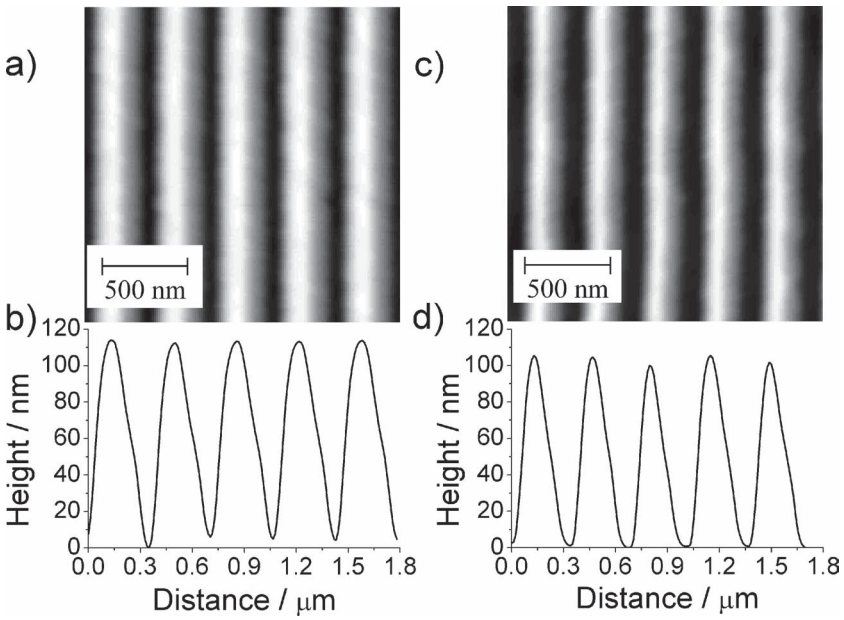

Figure 3. AFM images of the silicon master resonator (a) and the final UV-nanoimprinted structure (c) in the cured photoresist, along with the extracted height profiles (b and d, respectively).

Surface-emitting second-order distributed-feedback (DFB) lasers were made using sample **3** with the optimized molecular weight for ASE. The DFB resonators provide optical feedback in the plane of the polymer film via second-order Bragg scattering, and a surface emission normal to the film via first-order Bragg scattering, at wavelength λ_{Bragg} determined by $\lambda_{Bragg} = \Lambda n_{eff}$, where Λ is the corrugation period and n_{eff} is the effective refractive index of the waveguided optical mode.[1] The resonator structures were originally made by e-beam lithography on a silicon wafer, and transferred onto a silica substrate by a UV-NIL process in the resist mr-UVcur06 (Micro Resist Technology GmbH). The final structure of the nanoimprinted DFB resonator was analyzed and compared to the silicon master using scanning electron microscopy (SEM) and AFM. **Figure 3** shows a comparison of the surface profiles for the master and imprint structures, along with the corresponding extracted height profiles.

The master 1D photonic crystal structure had a period of 360 ± 10 nm and feature height of 110 ± 10 nm. In comparison, the final UV-NIL structures were measured to have a period of 340 ± 10 nm, with features of height 100 ± 10 nm. While the specific shape of the measured profile is influenced by the side angle of the AFM tip, the profiles show that the grating depth is well reproduced by the nanoimprint process. The small reduction (5%) in period is consistent with the film shrinkage previously reported for mr-UVCur06.[33]

The UV-NIL resist had a residual layer thickness of 300 nm, measured by surface profilometry. The BBEHP-PPV polymer film was deposited by spin-coating on top of the patterned resist layer. Films of thickness ranging from 446 to 593 nm were deposited on top of the corrugated resist (**Figure 4** shows SEM scans taken at a 45° angle of a cleaved laser device). The refractive index of the UV-NIL resist and BBEHP-PPV are respectively 1.53 and 1.64 at 530 nm, determined by variable-angle spectroscopic ellipsometry. A 1.5 μm thick top cladding layer of CYTOP (n = 1.35) was deposited on the BBEHP-PPV (Figure 4c), to give a more symmetrical mode profile in the waveguide, and to serve as an encapsulant and buffer between the LED and laser.

The distributed feedback lasers fabricated were optically excited using a commercial light-emitting diode (Philips Luxeon Rebel royal blue) emitting at 448 nm, overlapping well with the polymer's absorption spectrum. The LED was driven by a pulsed laser driver (PCO-7110-120-15, Directed Energy, Inc.) and produced a maximum optical output power density of 1000 W cm^{-2} with a pulse duration of 47 ns at a peak drive current of 100 A from a total light-emitting area of 1.3 mm by 1.3 mm.

As the electric current through the LED was increased, the emission intensity from the polymer showed a linear increase up to an optical excitation intensity of 770 W cm^{-2} where a change in the slope of the input-output curve signified the onset of lasing (**Figure 5**). At the same time a narrow (0.7 nm full width at half maximum, measurement resolution limited) peak appears in the output spectrum of the polymer laser at 533 nm, close to the wavelength of maximum optical gain. All measurements were carried out in air; using the CYTOP layer as an

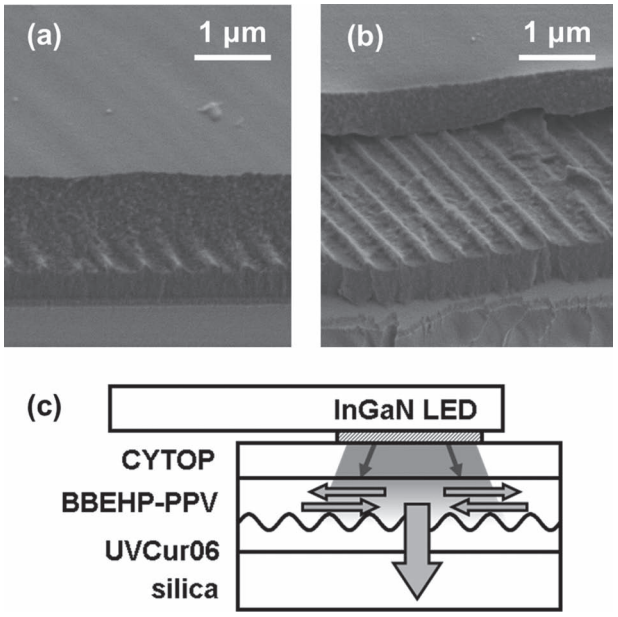

Figure 4. Side-view of a BBEHP-PPV light-emitting film spin-coated on a UV-nanoimprinted grating in photoresist on top of a glass substrate, taken at an angle of 45°. a) Cleaved edge showing the surface flatness and uniformity of the polymer film and the filling of the resonator structure. b) Peeled-back polymer film allows more of the resonator in the resist to be shown on top of the glass substrate. c) Schematic of LED-pumped laser.

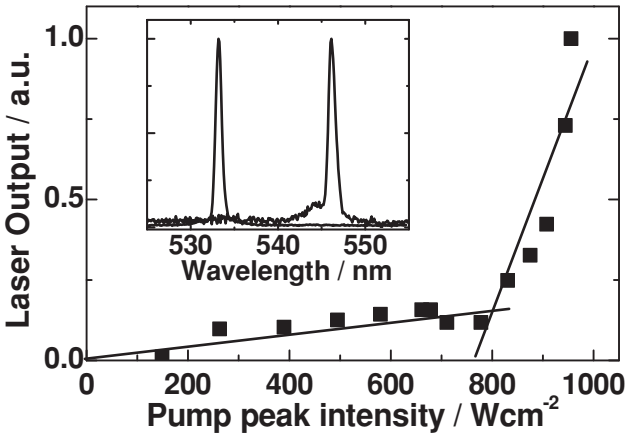

Figure 5. Input-output curve of a BBEHP-PPV UV-nanoimprinted laser pumped by a pulsed inorganic LED. The lines correspond to the operation below and above lasing threshold and are guides for the eye. Inset: Lasing spectra from two LED-pumped nanoimprinted organic lasers with BBEHP-PPV layers of 446 nm and 593 nm thickness.

encapsulant for the laser, no degradation was observed during the course of measurements.

The laser threshold density is higher than the measured ASE threshold above because of the smaller excitation region[30] available from LED pumping, and slower pulse rise time of the LED. Nevertheless, this is the lowest threshold density for a UV-NIL organic laser and enables for the first time a nanoimprinted laser to be LED-pumped, resulting in a compact and convenient laser source. The lowest threshold densities reported for organic lasers, fabricated by any room-temperature NIL process, are in the region of 8 kW cm^{-2} [22,23] and higher. There is one previous report of a similar threshold density (500 W cm^{-2}) for a hot-embossed organic laser,[26] however in that work the laser was pumped in the UV at 337 nm with a much longer excitation stripe (4 mm long). Such large areas and short wavelengths are not currently available from commercial high power LEDs.

By changing the thickness of the polymer film from 446 to 593 nm it was possible to tune the lasing wavelength across 12 nm, as shown in the inset to Figure 5. This tuning range was limited by the increase in laser threshold, for wavelengths longer and shorter than the peak ASE wavelength, above the maximum intensity possible from the LED. Under stronger optical excitation from the OPO used in the ASE measurements, the BBEHP-PPV lasers could be tuned from 522 nm to 558 nm. The organic laser showed a well-defined fan-shaped output beam, as expected for a one-dimensional distributed feedback resonator. The beam divergence was determined to be 11 mrad in the direction perpendicular to the grating lines (see Supporting Information), in good agreement with literature reports on the beam divergence of organic surface-emitting distributed feedback lasers.[34]

In conclusion we report the demonstration of LED-pumped organic semiconductor lasers simply fabricated by UV-nanoimprint lithography. The optical gain of the polymer gain medium was optimized by Soxhlet extraction of samples to reduce polydispersity and give low-loss thin-film waveguides with very low ASE thresholds. Nanoimprinted distributed feedback resonators were then combined with the light-emitting conjugated polymer with optimized gain properties to achieve nanoimprinted organic lasers with a lasing threshold of only 770 W cm^{-2}. These hybrid lasers incorporate a simple, scalable UV-nanoimprint lithography process compatible with mass-produced inorganic LEDs and therefore present a compact, inexpensive approach to integrated visible lasers.

Experimental Section

Polymer Synthesis: Following a path similar to a published synthesis route,[7] but using microwave-assisted Suzuki coupling with dioxaborolane (**1**) as a boronate, for the synthesis of the dihydroxy monomer building block (**2**) resulted in an improved yield of 86% (Scheme S1, Supporting Information). Using the standard catalyst tetrakis(triphenylphophine)Pd(0), which was freshly prepared from $PdCl_2$,[35] allowed better control of its quality and made the procedure more reproducible.

The samples used in this work were synthesized in four batches (**a**–**d**). In each, the final polymer was re-precipitated from THF: methanol (directly yielding samples **7** and **4** from synthesis batches **a** and **b**). To decrease the polydispersity index (PDI) after precipitation by methanol, the crude polymer (batches **b** and **c**) was subjected to Soxhlet extraction with methanol, acetone and dichloromethane for 24 hours each. The methanol extract was discarded whereas the acetone and dichloromethane fractions were evaporated and re-precipitated by dissolving in tetrahydrofuran and addition of methanol to produce the samples **1**, **5** and **6.**

In a separate batch **d**, the procedure of extracting with dichloromethane was interrupted after 12 hours, and the extract was evaporated and re-precipitated (THF-methanol). During the re-precipitation, two distinct forms of polymer were formed: 1) a fiber-like precipitate and 2) an amorphous powder-like solid. These were separated mechanically to give samples **3** and **8** respectively. For the remaining residue in the Soxhlet thimble, extraction was continued for another 12 hours, and after evaporation and re-precipitation sample **2** was afforded.

The molecular weight of the polymers was determined by multi-angle light scattering size exclusion chromatography using chloroform ($CHCl_3$) or tetrahydrofuran (THF) as an eluent. The values of dn/dc were assumed to be 0.161 ml g^{-1} for $CHCl_3$ and 0.184 ml g^{-1} for THF. The results are presented in Table 1.

Material Characterization: Thin polymer films of BBEHP-PPV, poly(2,5-bis(2',5'-bis(2"-ethylhexyloxy)phenyl)-*p*-phenylenevinylene), were spin coated from a chlorobenzene solution (20 mg ml^{-1}) on top of quartz substrates and absorption measurements were carried out on a Cary Varian 300 UV–vis absorption spectrometer. Photoluminescence measurements were performed using a Horiba Jobin Yvon Fluoromax 2 fluorimeter. Variable-angle spectroscopic ellipsometry measurements were performed on a J.A. Woolam Co. Inc. M-2000DI ellipsometer and the resulting data fitted using a Levenberg–Marquardt algorithm. Solid-state PLQYs were measured using a Hamamatsu Photonics C9920-02 absolute photoluminescence quantum yield measurement system.

For measurements of ASE, thin films of the polymer were spin-coated on quartz substrates and placed in a vacuum chamber (10^{-3} to 10^{-4} mbar pressure) for the duration of the measurement. The beam from a 4 ns pulsed optical parametric oscillator (Continuum Panther) operating at 430 nm was focused to a thin stripe (460 µm by 4.7 mm) on the surface of the film and the amplified waveguided fluorescence was detected at the edge of the film. The intensity and spectral width of the edge emission were recorded using a spectrograph with a cooled-CCD array (Jobin-Yvon Triax 180).

Resonator Fabrication: Distributed feedback resonators based on a periodic change of the waveguide effective index were created by a periodic corrugation of the UV-NIL layer. The grating period was Λ =

360 ± 10 nm to ensure feedback at the peak of the material's amplified spontaneous emission spectrum. Master gratings were defined using a Leo 1530/Raith Elphy Plus system in an electron-beam resist (ZEON ZEP 520A), which was spin-coated on top of a silicon wafer. The electron-beam resist was developed using xylene at 23 °C and the pattern (1 mm × 1 mm total area) was transferred into the silicon master using reactive ion etching (RIE) with a combination of SF_6 and CHF_3 gas (at a 1:1 ratio).

The resulting master structures were transferred onto a silica substrate using UV-nanoimprint lithography by creating a perfluoropolyether daughter stamp from the master structure and then using that as a mold for replicating the structures onto a photoresist (Micro Resist Technology UVCur06), spin-coated on top of a glass substrate that had been pretreated with an adhesion promoting agent (Micro Resist Technology mr-ASP1). The replication was performed using an EVG620 photomask aligner with custom tooling for UV-NIL using pressure (110 mbar) and under UV exposure (200 s at 15 mW cm^{-2} from a broadband mercury vapor lamp). The resulting gratings were imaged using a Veeco Caliber AFM with sharp AFM tip (Veeco SNL-10).

Supporting Information

Supporting Information is available from the Wiley Online Library or from the author.

Acknowledgements

The authors acknowledge support for this work from the Engineering and Physical Sciences Research Council (EPSRC) HYPIX project (grant number EP/F059922/1 and EP/F05999X/1). The authors thank EVGroup for process support for the UV-nanoimprint lithography, and Asahi Glass for the supply of CYTOP.

Received: December 12, 2012
Revised: March 7, 2013
Published online: April 12, 2013

[1] I. D. W. Samuel, G. A. Turnbull, *Chem. Rev.* **2007**, *107*, 1272.
[2] S. Chenais, S. Forget, *Polym. Int.* **2012**, *61*, 390.
[3] C. Grivas, M. Pollnau, *Laser Photonics Rev.* **2012**, *6*, 419.
[4] C. Vannahme, S. Klinkhammer, U. Lemmer, T. Mappes, *Opt. Express* **2011**, *19*, 8179.
[5] C. Vannahme, S. Klinkhammer, M. B. Christiansen, A. Kolew, A. Kristensen, U. Lemmer, T. Mappes, *Opt. Express* **2010**, *18*, 24881.
[6] A. Camposeo, P. Del Carro, L. Persano, D. Pisignano, *Adv. Mater.* **2012**, *24*, OP221.
[7] A. Rose, Z. G. Zhu, C. F. Madigan, T. M. Swager, V. Bulovic, *Nature* **2005**, *434*, 876.
[8] Y. Yang, G. A. Turnbull, I. D. W. Samuel, *Adv. Funct. Mater.* **2010**, *20*, 2093.
[9] T. Riedl, T. Rabe, H. H. Johannes, W. Kowalsky, J. Wang, T. Weimann, P. Hinze, B. Nehls, T. Farrell, U. Scherf, *Appl. Phys. Lett.* **2006**, *88*, 3.
[10] A. E. Vasdekis, G. Tsiminis, J. C. Ribierre, L. O'Faolain, T. F. Krauss, G. A. Turnbull, I. D. W. Samuel, *Opt. Express* **2006**, *14*, 9211.
[11] H. Sakata, H. Takeuchi, *Appl. Phys. Lett.* **2008**, *92*, 113310.
[12] S. Klinkhammer, X. Liu, K. Huska, Y. X. Shen, S. Vanderheiden, S. Valouch, C. Vannahme, S. Brase, T. Mappes, U. Lemmer, *Opt. Express* **2012**, *20*, 6357.
[13] Y. Yang, G. A. Turnbull, I. D. W. Samuel, *Appl. Phys. Lett.* **2008**, *92*, 163306.
[14] M. D. McGehee, M. A. Diaz-Garcia, F. Hide, R. Gupta, E. K. Miller, D. Moses, A. J. Heeger, *Appl. Phys. Lett.* **1998**, *72*, 1536.
[15] C. Kallinger, M. Hilmer, A. Haugeneder, M. Perner, W. Spirkl, U. Lemmer, J. Feldmann, U. Scherf, K. Müllen, A. Gombert, V. Wittwer, *Adv. Mater.* **1998**, *10*, 920.
[16] L. J. Guo, *Adv. Mater.* **2007**, *19*, 495.
[17] S. Y. Chou, P. R. Krauss, P. J. Renstrom, *Science* **1996**, *272*, 85.
[18] L. M. Goldenberg, V. Lisinetskii, Y. Gritsai, J. Stumpe, S. Schrader, *Adv. Mater.* **2012**, *24*, 3339.
[19] E. H. Cho, H. S. Kim, B. H. Cheong, P. Oleg, W. Xianyua, J. S. Sohn, D. J. Ma, H. Y. Choi, N. C. Park, Y. P. Park, *Opt. Express* **2009**, *17*, 8621.
[20] S. H. Ahn, L. J. Guo, *Adv. Mat.* **2008**, *20*, 2044.
[21] M. Berggren, A. Dodabalapur, R. E. Slusher, A. Timko, O. Nalamasu, *Appl. Phys. Lett.* **1998**, *72*, 410.
[22] Y. Chen, Z. Li, Z. Zhang, D. Psaltis, A. Scherer, *Appl. Phys. Lett.* **2007**, *91*, 051109.
[23] E. Mele, A. Camposeo, R. Stabile, P. Del Carro, F. Di Benedetto, L. Persano, R. Cingolani, D. Pisignano, *Appl. Phys. Lett.* **2006**, *89*, 131109.
[24] K. Yamashita, N. Takeuchi, K. Oe, H. Yanagi, *Opt. Lett.* **2010**, *35*, 2451.
[25] J. R. Lawrence, G. A. Turnbull, I. D. W. Samuel, *Appl. Phys. Lett.* **2003**, *82*, 4023.
[26] M. Ichikawa, Y. Tanaka, N. Suganuma, T. Koyama, Y. Taniguchi, *Jap. J. Appl. Phys.* **2003**, *42*, 5590.
[27] M. B. Christiansen, M. Scholer, A. Kristensen, *Opt. Express* **2007**, *15*, 3931.
[28] D. Pisignano, L. Persano, E. Mele, P. Visconti, M. Anni, G. Gigli, R. Cingolani, L. Favaretto, G. Barbarella, *Synth. Met.* **2005**, *153*, 237.
[29] M. G. Ramirez, P. G. Boj, V. Navarro-Fuster, I. Vragovic, J. M. Villalvilla, I. Alonso, V. Trabadelo, S. Merino, M. A. Díaz-García, *Opt. Express* **2011**, *19*, 22443.
[30] E. M. Calzado, J. M. Villalvilla, P. G. Boj, J. A. Quintana, V. Navarro-Fuster, A. Retolaza, S. Merino, M. A. Díaz-García, *Appl. Phys. Lett.* **2012**, *101*, 223303.
[31] K. Koynov, A. Bahtiar, T. Ahn, R. M. Cordeiro, H. H. Horhold, C. Bubeck, *Macromolecules* **2006**, *39*, 8692.
[32] M. Anni, A. Perulli, G. Monti, *J. Appl. Phys.* **2012**, *111*, 093109.
[33] S. Takei, *Appl. Phys. Express* **2010**, *3*, 025202.
[34] G. A. Turnbull, P. Andrew, W. L. Barnes, I. D. W. Samuel, *Appl. Phys. Lett.* **2003**, *82*, 313.
[35] D. R. Coulson, L. C. Satek, S. O. Grim, *Inorg. Synth.* **1972**, *13*, 121.